# Supplementary Material

Mechanistic Insight in Phase Transfer Agent Assisted Ultrasonic Desulfurization

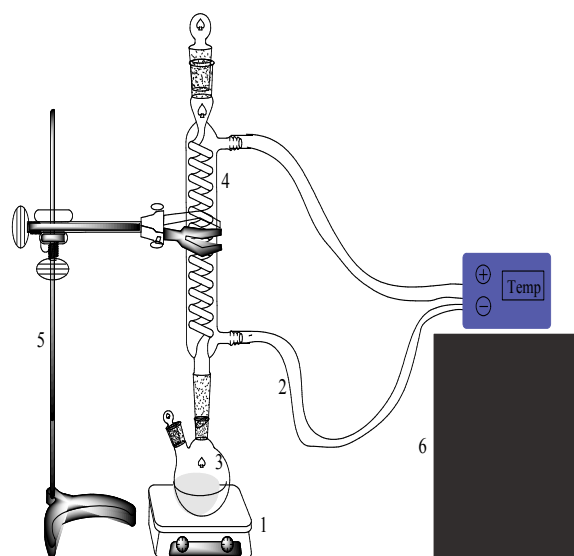Jaykumar B. Bhasarkar[1], Mohit Singh[2], Vijayanand S. Moholkar[1,*]

[1] Department of Chemical Engineering, Indian Institute of Technology Guwahati, Guwahati – 781039, Assam, India

[2] Department of Chemical Engineering, National Institute of Technology Tiruchirapalli, Tiruchirapalli - 620015, Tamil Nadu, India
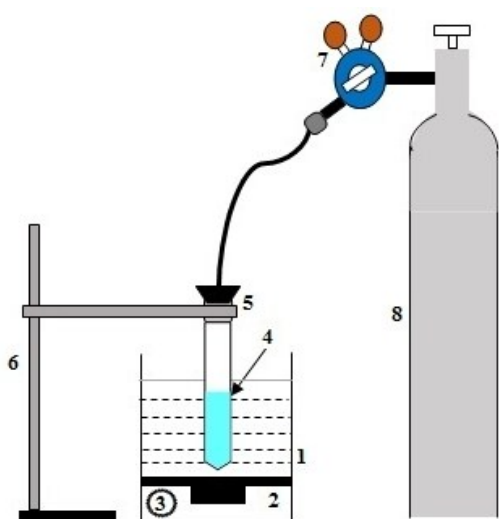
Fig. S.1a: Experimental setup for ultrasound system

Fig. S.1b: Experimental setup for mechanical stirring

Legends (fig. S.1a): 1. Ultrasound bath; 2. Transducer; 3. Controller or regulator; 4. Reaction mixture; 5. Test tube with rubber cork; 6. Burette stand; 7. Pressure regulator; 8. N_2 gas cylinder

Legends (fig. S.1b): 1 – Magnetic stirrer, 2 – Silicon pipe, 3 – Round bottom flask containing reaction mixture, 4 – Condenser, 5 – Holding stand, 6 – Temperature controllers

Preliminary Experiments for Determination of Composition of Reaction Mixture

Preliminary experiments were carried out to identify the optimum quantities of phase transfer agent (PTA), TBAB. Another optimization parameter was the temperatures of the reaction mixture, which play an important role in DBT oxidation reaction. As far as other experimental parameters such as volume ratio of organic to aqueous phase and optimum composition of peracetic acid (quantities of acetic acid and H_2O_2) and performic acid (quantities of formic acid and H_2O_2) are concerned, we have used the results of our earlier studies.[1,2]

Optimization of Quantity of Phase Transfer Agent: The results of effect of quantity of phase transfer agent, tetrabutyl ammonium bromide (TBAB), on DBT reduction (or desulfurization efficiency) are shown in Fig. S.2. The other experimental parameters have been given in the figure caption. The amount of PTA (TBAB) added to reaction solution was varied in the range of 0.25–1.0 g. Extent of DBT oxidation showed sharp proportionate rise with amount of PTA in the reaction mixture increasing from 0 to 0.5 g. However, increase of PTA quantity from 0.5 to 0.75 g did not show any marked increase in the oxidation efficiency. Further rise in PTA quantity (from 0.75 to 1.0 g) reduced the extent of oxidation. On the basis of these results, we have taken as a 0.5 g phase transfer agent optimum dose for further experiments.
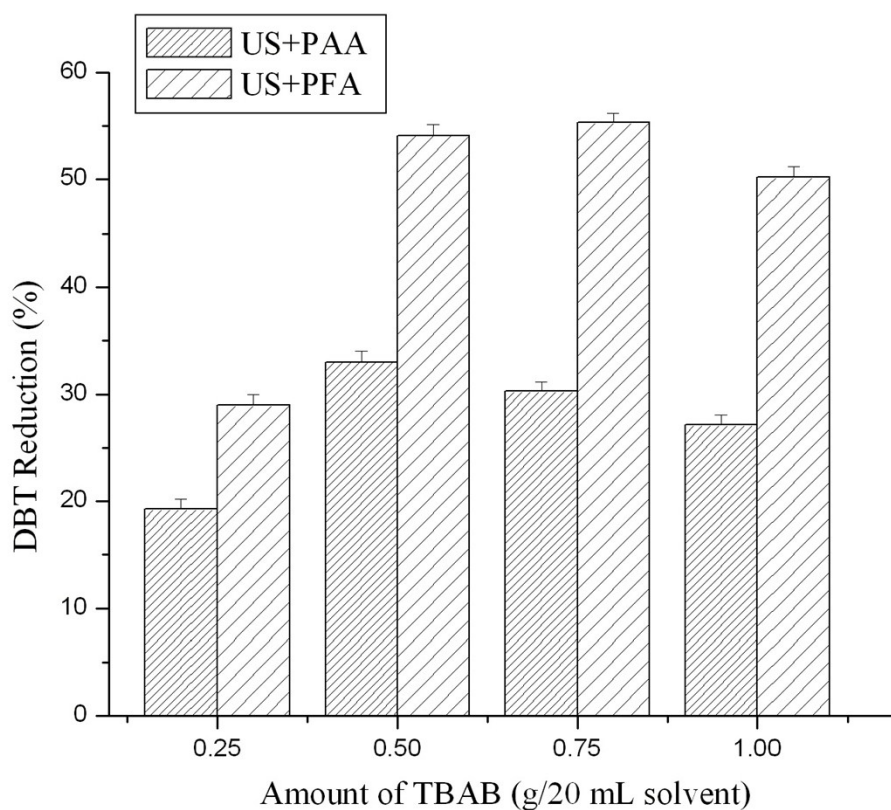
Fig. S.2. Effect of PTA dose on DBT reduction
Other parameters for experiment: solvent: toluene = 20 mL, oxidant: PFA - Performic acid (formic acid = 4 mL, H_2O_2 = 2 mL) = 6 mL; PAA - Peracetic acid (acetic acid = 4 mL, H_2O_2 = 2mL) = 6 mL; Temperature = 303 K

Effect of temperature: The effect of temperature on extent of oxidative desulfurization in ultrasound system and mechanical stirred system is shown in Fig. S.3. The range of temperature for optimization of oxidative desulfurization was 30°–60°C for ultrasound and mechanical stirring. The oxidant used in all experiments was performic acid with TBAB as a phase transfer agent. The DBT removal rate increase with increasing in temperature. Sufficiently high removal rates are obtained upto 40°C in ultrasound system because of the intense emulsification with generation of high interfacial area due to ultrasound. This effect helps overcome the mass transfer limitations due to which the reaction kinetics increases. For temperature higher than 40°C, the intensity of transient cavitation is reduced due to large

evaporation of solvent vapor in the cavitation bubble which later on cushions its collapse. In case of mechanical stirring, the oxidation efficiency shows marked rise for temperature range of 30°-40°C, and relatively lesser rise till 60°C. Another factor that contributes to this effect is decomposition of H_2O_2 to H_2O and O_2 at higher temperature. On the basis of these results, we have considered 40°C as the optimum temperature for ultrasound treatment while 60°C as the optimum temperature for mechanical stirring.
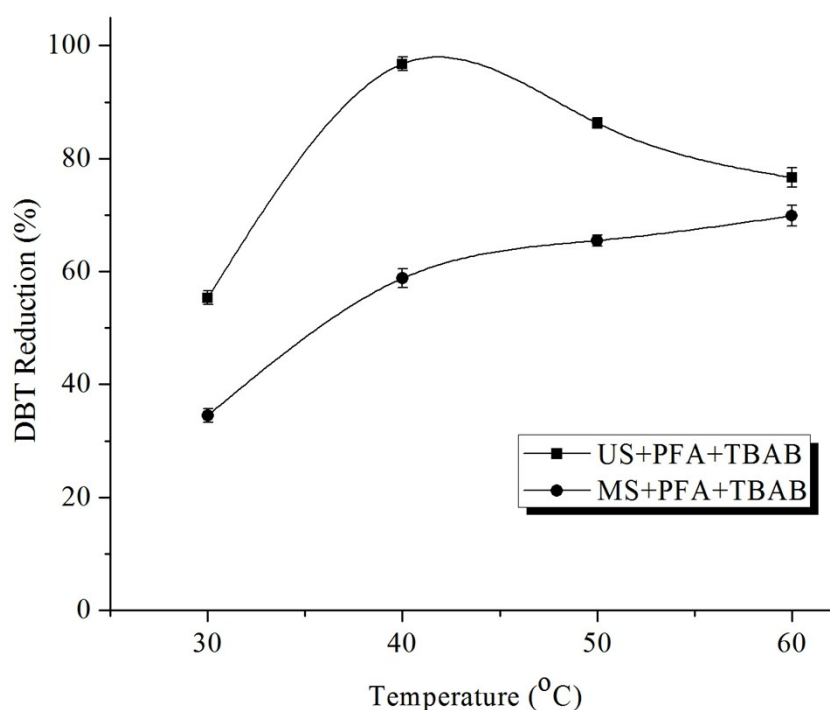
Fig. S.3: Temperature effect on DBT reduction for US and MS system
Other parameter: Solvent – toluene, Oxidant: performic acid + TBAB as PTA

References

1. J. B. Bhasarkar, S. Chakma and V. S. Moholkar, *Ind. Eng. Chem. Res.,* 2013, **52**, 9038–9047.
2. J. B. Bhasarkar, S. Chakma and V. S. Moholkar, *Ultrason. Sonochem.*, 2015, **24**, 98–106.

Table S.1: Experimental categories with exact composition of reaction mixture

Experimental Category	Molar Ratio $\frac{H_2O_2}{HCOOH}$	Molar Ratio $\frac{H_2O_2}{PTA}$	Volume Ratio $\frac{Solvent \; \#}{Oxidant}$
A.1 US + H_2O_2 + HCOOH (4 mL) [PFA]	0.6	16.11	3.33
A.2 MS+ H_2O_2 + HCOOH (4 mL)	0.6	16.11	3.33
B.1 US +PFA + TBAB (50 mg)	0.6	16.11	3.33
B.2 MS +PFA + TBAB (50 mg)	0.6	16.11	3.33
C. US + PFA+ TBAB + ESP (1.8 bar)	0.6	16.11	3.33

Note: In each of the experimental categories A, B, and C, the total volume of solvent (or model fuel) used is 20 mL.
- Decided on the basis of optimization experiments (Bhasarkar et al., 2013, 2015)

Bhasarkar JB, Chakma S, Moholkar VS. Mechanistic features of oxidative desulfurization using sono–fenton–peracetic acid (Ultrasound/ Fe^{2+}– CH_3COOH–H_2O_2) system. *Ind. Eng. Chem. Res.* 2013;52:9038–9047.
Bhasarkar JB, Chakma S, Moholkar VS. Investigations in physical mechanism of the oxidative desulfurization process assisted simultaneously by phase transfer agent and ultrasound. *Ultrason. Sonochem.* 2015;24:98–106.

Table S.2. Model for the Radial Motion of Cavitation Bubble

| Model Component	Equation	Initial Value
1. Radial motion of the cavitation bubble	$$\left(1-\frac{dR/dt}{c}\right)R\frac{d^2R}{dt^2}+\frac{3}{2}\left(1-\frac{dR/dt}{3c}\right)\left(\frac{dR}{dt}\right)^2 = \frac{1}{\rho_L}\left(1+\frac{dR/dt}{c}\right)(P_i-P_t)+$$ $$\frac{R}{\rho_L c}\frac{dP_i}{dt}-4\nu\frac{dR/dt}{R}-\frac{2\sigma}{\rho_L R}$$ Internal pressure in the bubble: $P_i = \dfrac{N_{tot}(t)\,kT}{\left[4\pi\left(R^3(t)-h^3\right)/3\right]}$ Pressure in bulk liquid medium: $P_t = P_0 - P_A\sin(2\pi ft)$	At $t = 0$, $R = R_o$ $dR/dt = 0$
2. Diffusive flux of toluene molecules	$$\frac{dN_{TOL}}{dt}=4\pi R^2 D_{TOL}\left.\frac{\partial C_{TOL}}{\partial r}\right|_{r=R}\approx 4\pi R^2 D_{TOL}\left(\frac{C_{TOL,R}-C_{TOL}}{l_{diff}}\right)$$ Instantaneous diffusive penetration depth: $$l_{diff}=\min\left(\sqrt{\frac{RD_{TOL}}{|dR/dt|}},\frac{R}{\pi}\right)$$	At $t = 0$, $N_{TOL} = 0$
3. Heat conduction across bubble wall	$$\frac{dQ}{dt}=4\pi R^2\lambda\left.\frac{\partial T}{\partial r}\right|_{r=R}\approx 4\pi R^2\lambda\left(\frac{T_0-T}{l_{th}}\right)$$ Thermal diffusion length: $l_{th}=\min\left(\sqrt{\dfrac{R\kappa}{|dR/dt|}},\dfrac{R}{\pi}\right)$	At $t = 0$, $Q = 0$
4. Overall energy balance	$C_{V,mix}dT/dt = dQ/dt - P_i dV/dt + (h_{TOL}-U_{TOL})dN_{TOL}/dt$ Mixture heat capacity: $C_{V,mix}=\sum C_{V,i}N_i$ ($i = N_2/O_2/$toluene) Molecular properties of toluene: Enthalpy: $h_{TOL}=4kT_o$ Internal energy: $U_{TOL}=N_{TOL}kT\left(3+\sum_{i=1}^{3}\dfrac{\theta_i/T}{\exp(\theta_i/T)-1}\right)$ Heat capacity of various species ($i = N_2/O_2/$toluene): $C_{V,i}=N_i k\left(f_i/2+\sum\left((\theta_i/T)^2\exp(\theta_i/T)\big/(\exp(\theta_i/T)-1)^2\right)\right)$	At $t = 0$, $T = T_o$

Notation: c – velocity of sound in bulk liquid medium, C_{TOL} – concentration of toluene molecules in the bubble, $C_{TOL,R}$ – concentration of toluene molecules at the bubble wall or gas–liquid interface, $C_{V,i}$ – heat capacity at constant volume for species i, dR/dt – bubble wall velocity, D_{TOL} – diffusion coefficient of toluene vapor, f – frequency of ultrasound wave, f_i – translational and rotational degrees of freedom, h – van der Waal's hard core radius, h_{TOL} – molecular enthalpy of toluene, k_b – Bolzmann constant, N_{N2} – number of nitrogen molecules in the bubble, N_{O2} – number of oxygen molecules in the bubble, N_{TOL} – number of toluene molecules in the bubble, N_{tot} – total number of molecules (gas + vapor) in the bubble, P_A – pressure amplitude of ultrasound wave, P_o – ambient (bulk) pressure in liquid, Q – heat conducted across bubble wall, R – radius of the bubble, T – temperature of the bubble contents, t – time, T_o – ambient (or bulk liquid medium) temperature, U_{TOL} – internal energy of toluene molecules, V_b – volume of the bubble, V_{turb} – velocity of microturbulence, ρ_L – density of the liquid, ν – kinematic viscosity of liquid, σ – surface tension of liquid, λ – thermal conductivity of bubble contents, κ – thermal diffusivity of bubble contents, θ – characteristic vibrational temperature(s) of the species.

Table S.3. Thermodynamic Properties of Various Species[#]

| Species	Degrees of freedom (translational + rotational) (f_i)	Lennard–Jones force constants		Characteristic vibrational temperatures θ (K)
		σ (10^{-10} m)	ε/k (K)	
N_2	5	3.68	92	3350
O_2	5	3.43	113	2273
Toluene	6	5.82	450.7	1004.13, 1055.81, 2111.63, 2163.31, 2325.74, 4224.08, 4375.02

 # *Data source:* 1. R. C. Reid, J. M. Prausnitz and B. E. Poling, McGraw−Hill, New York, 1987. 2. J. O. Hirschfelder, C. F. Curtiss and R. B. Bird, Wiley, New York, 1954. 3 E. U. Condon and H. Odishaw, McGraw−Hill, New York, 1958. 4. J. Zhou, X. Lu, Y. Wang and J. Shi, *Fluid Phase Equilib.*, 2000, **172**, 279–291. 5. Y. Zhu, X. Lu, J. Zhou, Y. Wang and J. Shi, *Fluid Phase Equilib.*, 2000, **194−197**, 1141–1159.

Note: Diffusion of non–condensable gas across bubble interface during radial motion is ignored in the present model as the time scale for the diffusion of gases is much higher than the time scale for the radial motion of bubble. The model equations have been solved using Runge–Kutta adaptive step size method (Ref: W. H. Press, S. A. Teukolsky, B. P. Flannery and W. T. Vetterling, Cambridge University Press, New York, 1992).
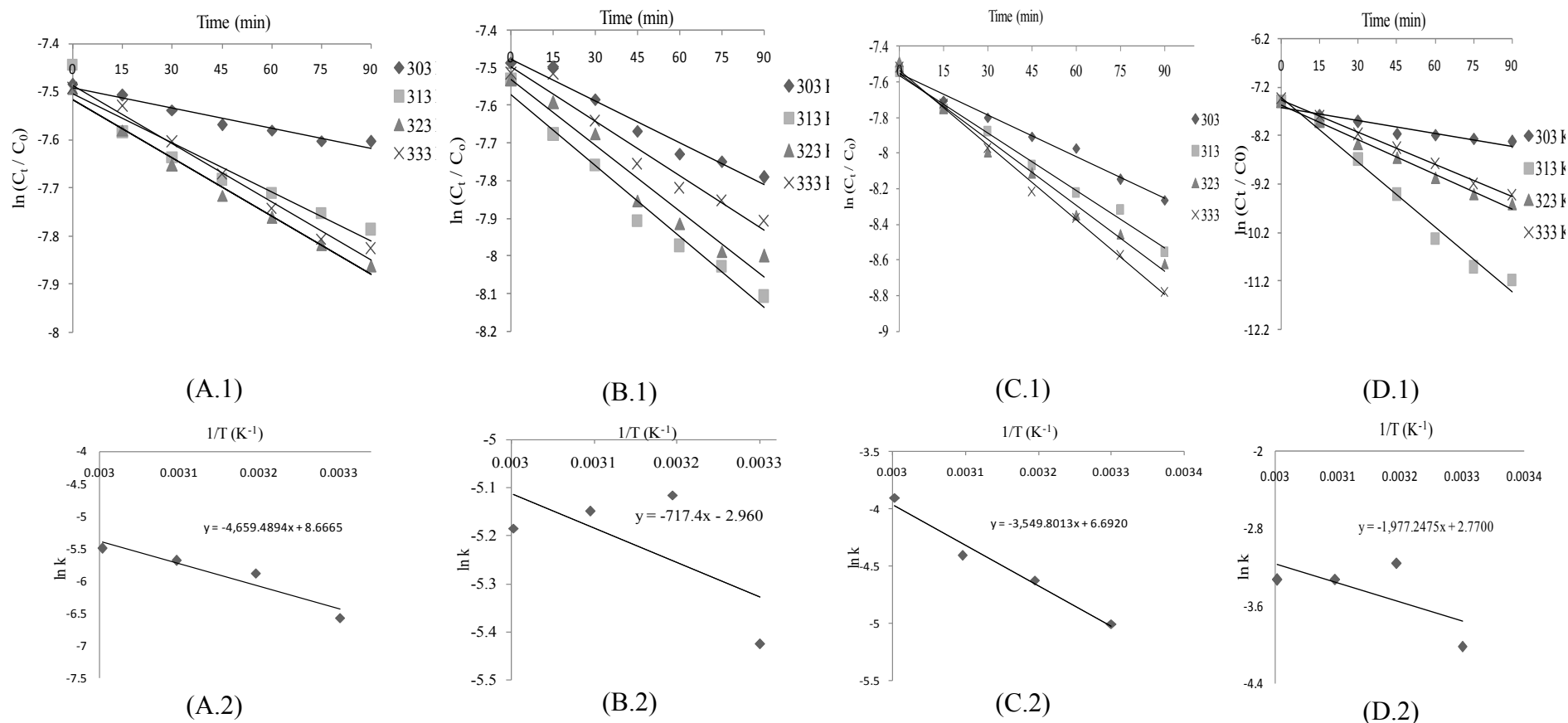
Fig. S.4: Kinetic analysis of oxidative desulfurization under ultrasound treatment and mechanical stirring using performic acid as oxidant coupled with TBAB as phase transfer agent. (A.1) 1st order fit of the experimental data for mechanical stirring + PFA treatment; (A.2) Arrhenius plot for the mechanical stirring + PFA treatment; (B.1) 1st order fit of the experimental data for ultrasound + PFA treatment; (B.2) Arrhenius plot for the ultrasound + PFA treatment, (C.1) 1st order fit of the experimental data for mechanical stirring + PFA + PTA; (C.2) Arrhenius plot for the mechanical stirring + PFA + PTA, (D.1) 1st order fit of the experimental data for only ultrasound treatment + PFA + PTA; (D.2) Arrhenius plot for the only ultrasound treatment + PFA + PTA.
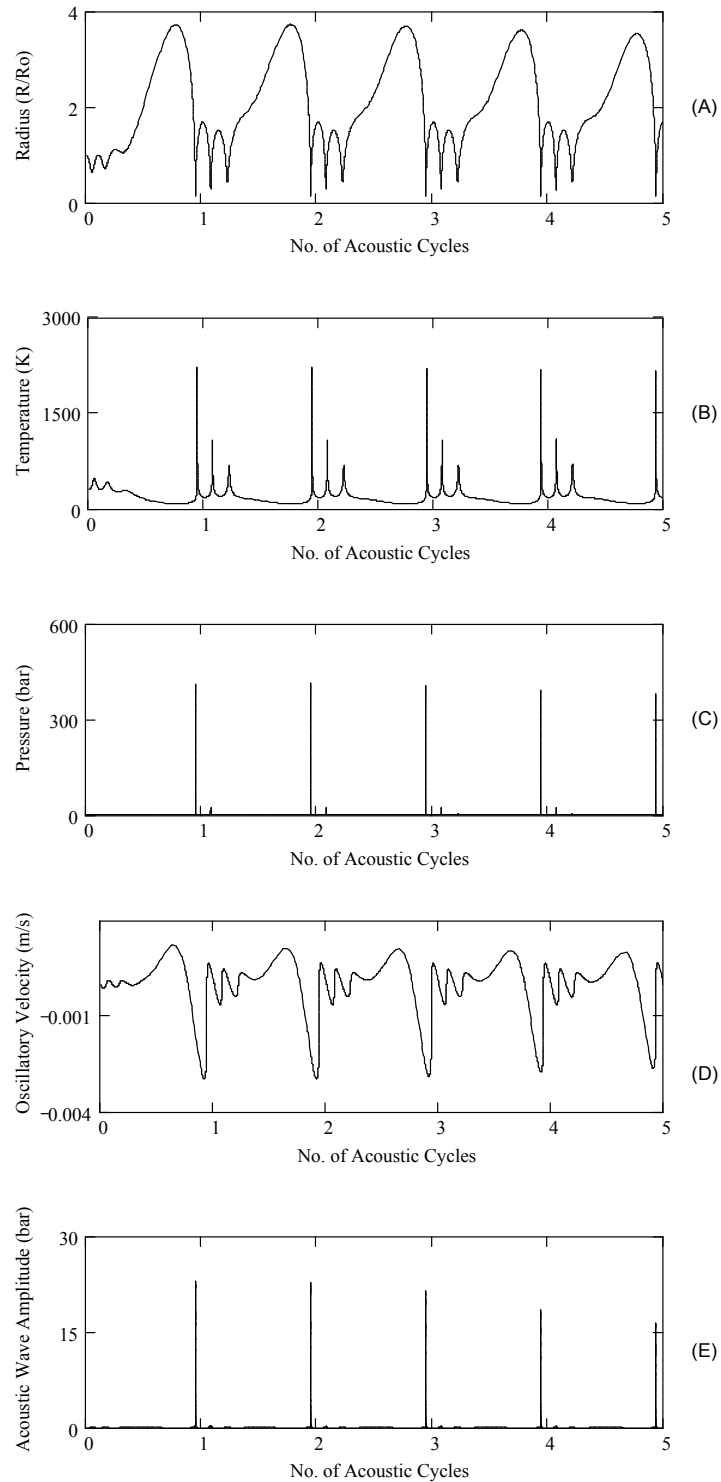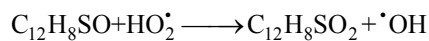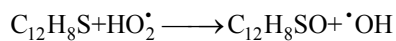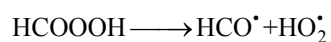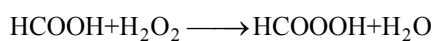
Fig. S.5. Simulations of radial motion of a 5 micron air bubble in toluene at atmospheric static pressure. Time history of (A) radius of the bubble; (B) temperature inside the bubble; (C) pressure inside the bubble; (D) microturbulence generated by the bubble; (E) acoustic waves emitted by the bubble.
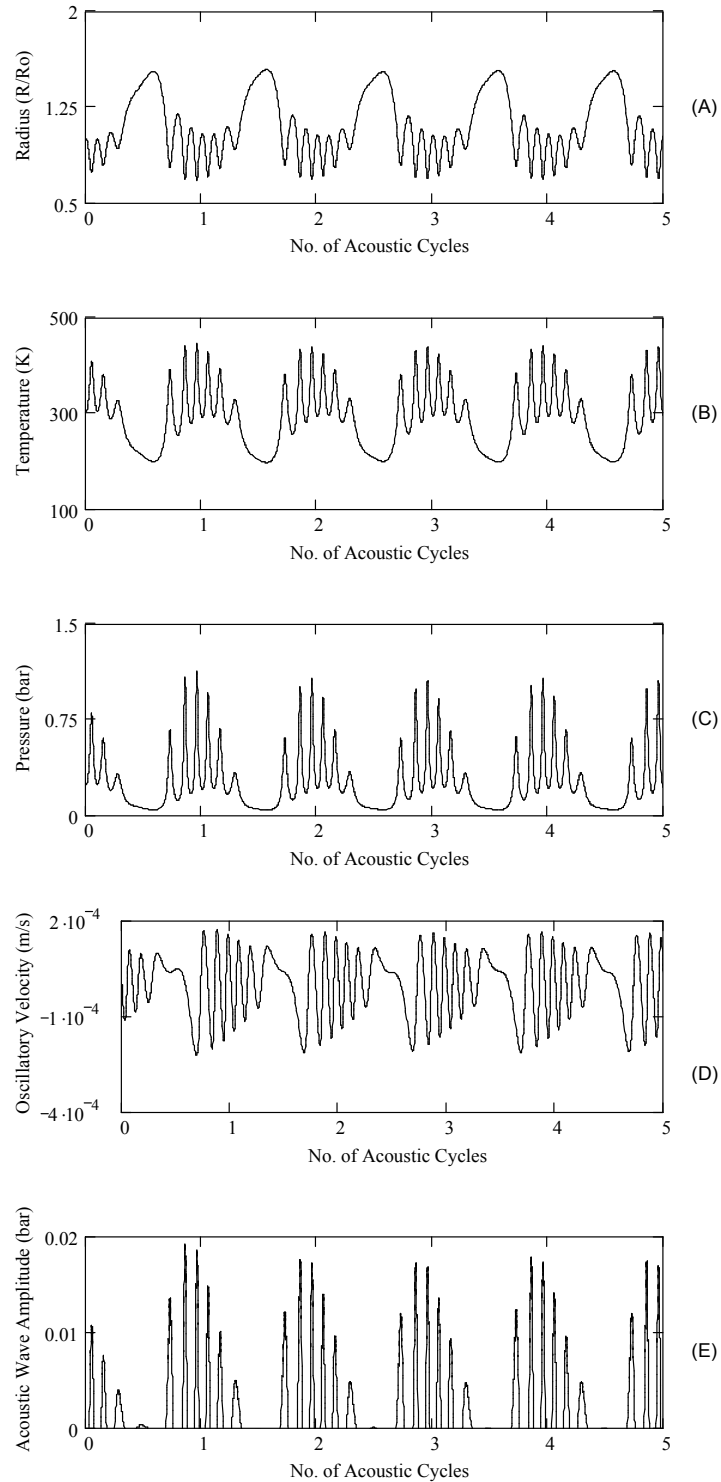
Fig. S.6: Simulations of radial motion of a 5 micron air bubble in toluene at elevated static pressure of 1.6 bar. Time history of (A) radius of the bubble; (B) temperature inside the bubble; (C) pressure inside the bubble; (D) microturbulence generated by the bubble; (E) acoustic waves emitted by the bubble.
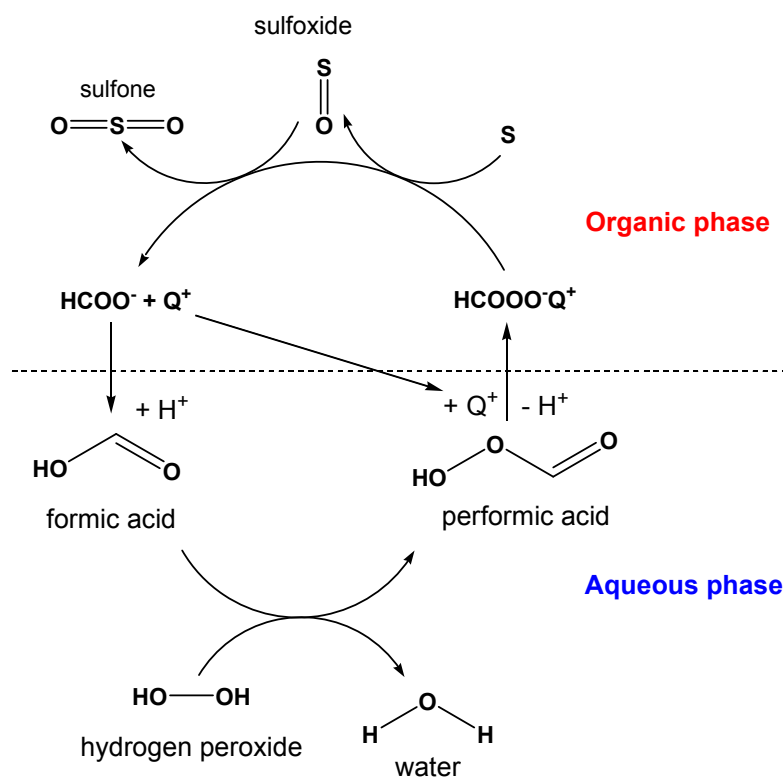
Scheme S.1: The cyclic mechanism of phase transfer agent (PTA) during oxidative desulfurization with performic acid

$$HCOOH + H_2O_2 \longrightarrow HCOOOH + H_2O$$

$$HCOOOH \longrightarrow HCO^\bullet + HO_2^\bullet$$

$$C_{12}H_8S + HO_2^\bullet \longrightarrow C_{12}H_8SO + {}^\bullet OH$$

$$C_{12}H_8SO + HO_2^\bullet \longrightarrow C_{12}H_8SO_2 + {}^\bullet OH$$

Scheme S.2: Reaction mechanism for performic acid induced oxidative desulfurization